Fully biobased, elastomeric and compostable random copolyesters of poly(butylene succinate) containing Pripol 1009 moieties: Structure-property relationship

26 November 2024

Fully biobased, elastomeric and compostable random copolyesters of poly(butylene succinate) containing Pripol 1009 moieties: structure-property relationship

Silvia Quattrosoldi 1†, Michelina Soccio 1†*, Massimo Gazzano 2‡, Nadia Lotti 1†*, Andrea Munari 1†

1† Dipartimento di Ingegneria Civile, Chimica, Ambientale e dei Materiali Università di Bologna, Via Terracini, 28, 40131 Bologna, Italy

2‡Istituto per la Sintesi Organica e la Fotoreattività, CNR, Via Gobetti 101, 40129 Bologna, Italy

ABSTRACT

Fully biobased random copolymers of poly(butylene succinate) (PBS) containing different amount of Pripol 1009 moieties were synthesized by melt poycondensation. Molecular characterization confirmed the chemical structure and the random distribution of counits (NMR) and indicated that high molecular weight samples were obtained (GPC). All the polymers under study were semicrystalline, developing the typical α-PBS crystalline phase, the melting temperature and the crystallinity degree regularly decreasing with the increase of Pripol content. Pripol moieties determined also an improvement of polymer chain flexibility, as proved by the glass transition temperature decreasing, and of thermal stability. Polymer mechanical response was nicely tuned by changing copolymer composition, the copolymer with the highest Pripol content showing the typical behavior of thermoplastic elastomers despite its random nature. Lastly, biodegradation rate in compost also increased with the content of Pripol due to the parallel decrease of sample crystallinity degree. Surprisingly, microorganisms present in the compost preferentially attack BS comonomeric units despite their semicrystalline nature.

INTRODUCTION

Succinic acid (SA) is a C4 dicarboxylic acid obtainable both from fossil (hydrogenation of maleic anhydride) and renewable resources (from glucose, sucrose and biobased glycerol).[1–4] According to U.S. Department of Energy, it can be considered one of the twelve most promising chemical biobased building blocks, with an estimated market value of 57 million €, of which 34% consumed in Europe, the largest market. Biobased succinic acid has also the advantage of capturing CO_2, 1 tons of SA being able to bond 4.5 – 5 tons of CO_2.[5]

SA is a very versatile building block for a broad range of applications, from high-value niche applications, such as personal care products and food additives, to large volume applications, such as bio-polyesters, polyurethanes, resins and coatings. More precisely, it can be mentioned production of poly(butylene succinate), poly(butylene succinate-terephthalate) copolyester (9%) and polyester polyols (6.2%), use in food industry as acidulant, flavor enhancer and sweetener (12.6%), in the pharmaceutical industry (15.1%), and in the production of resins, coatings and pigments (19.3%).[6,7] For all the reasons mentioned above, the forecasted growth of the bio-based SA market is expected to register a CAGR of over 35% by 2023.

Poly(butylene succinate) (PBS) is a biodegradable and compostable (according to DIN EN 13432) polyester, obtainable from succinic acid (SA) and 1,4-butanediol (BD). In the past, it was exclusively prepared from fossil raw materials, but today can be synthesized 100% biobased, starting from bio-SA e bio-BD.[8,9] The use of SA and BD from renewable resources reduces PBS carbon footprint, the greenhouse gas emissions (GHG) decreasing by ca. 50% to 80% compared to the fossil counterpart.[10]

PBS is a semicrystalline polyester with a melting temperature over 100°C, workable at temperatures up to ca. 200°C and with properties similar to LDPE.[11] PBS has a wide processing/temperature window and is suitable for extrusion, injection molding, thermoforming, fiber spinning and film blowing. By these conventional processing techniques, PBS is used in different fields, such as electronics,[12–14]food packaging,[15–17], agricultural mulch films,[18–20], hygiene products,[21] etc.

In the last ten years, PBS has been the subject of in-depth studies by the academy, as evidenced by the copious publication of scientific articles.[22-28] In particular, PBS has proved to be a promising material both for biomedical applications,[29-35] such as controlled drug release systems[36-38] and supports for tissue engineering[29,30,36,39-46] and environmental ones [47-56] thanks to its good thermo-mechanical properties, biocompatibility[29,30,36,39,41-44,46,57] and biodegradability, this last proved both in compost,[52,58,59] presence of enzymes[60-67] and under physiological conditions.[42-46,68,69]

Nevertheless, it cannot be employed for those applications requiring very soft materials or very fast degrading polymers.

As it is well known, the unsatisfactory properties of a polymer can be improved through different strategies, able to preserve at the same time the already good ones: we are referring to physical and reactive blending,[24,70-73] copolymerization[74-77] and preparation of composites and nanocomposites.[78-82] The authors of this article have been active for a long time in the chemical modification of PBS by copolymerization. In particular, the chemical structure of PBS has been modified by inserting co-units containing heteroatoms (in particular oxygen and sulfur)[43-46,52,65-68,83-85], branches[51] and highly flexible co-units into the chain.[53] To tailor the final properties, we have acted both on the type and on the quantity of the comonomer as well as on the architecture of the resulting copolymer (statistical rather than block arrangement of comonomeric units).

Croda has been selling for some time a series of products obtained from renewable sources, among these Pripol 1009, currently used in adhesives, engineered plastics and elastomers to improve the final product flexibility, thermo-oxidative stability and hydrolysis and chemical resistance. Pripol 1009 is a fatty diacid containing an aliphatic 6 carbon atoms ring connected to the -COOH groups through PE-like segments and presenting quite long side branches too. Besides as additive, Pripol 1009 can be also used as comonomer in the synthesis of copolyesters in which, both the main and lateral aliphatic chains of Pripol structure, can enhance the final polymer chain flexibility. Moreover, the use of Pripol 1009 as co-unit allows to reduce the -COOR- density along the macromolecular backbone thus limiting the ester linkage hydrolysis and thermal degradation. Finally, the introduction of a such bulky moiety can deeply affect and reduce the crystallization capability of the reference homopolymer further expanding the final material applications.

With the aim of enhancing and mainly tuning PBS final properties, broadening its applicability both in soft tissue engineering as well as for sustainable flexible packaging, random copolymers have been prepared by insertion along its macromolecular chains of different amounts of Pripol 1009. Final material properties have been correlated with composition and structure-property relationship have been extrapolated.

METHODS AND MATERIALS

MATERIALS Succinic acid (SA), butanediol (BD), and Ti(OBu)$_4$ (TBT) were purchased by Aldrich. Pripol 1009 is a commercial fully biobased diacid kindly provided by Croda Italiana S.p.A. (structure in the following).

HOOC ⌇⌇⌇⌇ COOH

(CH$_2$)$_n$ n = 6/7/8

(CH$_2$)$_n$ CH$_3$

CH$_3$
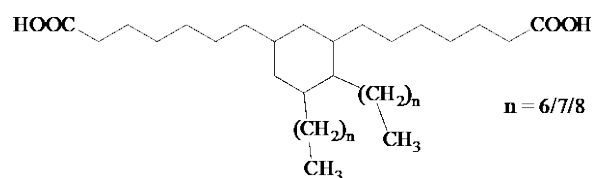
Pripol 1009 chemical structure.

SYNTHESIS PBS random copolymers were synthesized through the well-known bulk two-step polycondensation process, starting from a mixture with different SA/Pripol1009 ratio, BD, this last used with a 30 mol% excess, and TBT (200 ppm). The reagents, together with the catalyst, were charged in a thermostated and continuously stirred glass reactor. The first step was carried out in inert atmosphere at 180 °C. During this phase, which lasts 90 min, the esterification reactions take place with the release of water molecules. In the second stage, the temperature is increased till 220 °C and the pressure is progressively reduced to 0.1 mbar, to favor the polycondensation reactions and consequently the molecular weight growth. The polymerization process was stopped when a constant torque value was measured, indicating a stable molecular weight has been reached.

MOLECULAR CHARACTERIZATION The chemical structure, composition and randomness degree have been determined by ^{1}H-NMR and ^{13}C-NMR spectroscopy. The samples were dissolved (5 and 40 mg ml^{-1} for ^{1}H- and ^{13}C-NMR, respectively) in chloroform-d solvent with tetramethylsilane (0.03 vol.%) as internal standard. The measurements were carried out at 25 °C, employing Varian INOVA 400 MHz instrument.

Molecular weight was determined by gel-permeation chromatography (GPC) at 30°C using a 1100 Hewlett Packard system equipped with PL gel 5μ MiniMIX-C column. Refractive index was employed as detector. Chloroform was used as eluent (0.3 mL min^{-1} flow) of polymer solution (2 mg ml^{-1}). The calibration curve was obtained with monodisperse polystyrene standards in the range of 2000-100000 g mol^{-1}.

FILM PREPARATION Before further characterization, all the samples were compression molded (Carver C12 press). The as-synthesized polymers were put into two Teflon plates and heated till a temperature T = T_m + 40 °C under a pressure of 2 ton/m^2 kept for 3 min and allowed to cool to room temperature. Films of about 70 μm thickness have been prepared following this protocol.

THERMAL ANALYSIS The characteristic temperatures were determined by Differential Scanning Calorimetry (DSC) measurements using a Perkin Elmer DSC6 Instrument equipped with intracooler set at -70 °C. The samples were subjected to the following treatment in nitrogen atmosphere:

Heating step from –70 °C to T_m + 40 °C at 20°C min^{-1} (first scan).

Isothermal step of 3 min.

Cooling step to -70 °C at 100 °C min^{-1}

Heating step from –70 °C to T_m + 40 °C at 20°C min^{-1} (second scan).

Glass transition temperature (T_g) was taken at half-height of the glass to rubber transition step with the corresponding ΔC_p calculated from the step height, while melting temperature (T_m) was taken at the peak maximum of the melting endotherm with the corresponding ΔH_m calculated from the area under the peak.

The thermal stability has been evaluated by a Perkin Elmer TGA4000 analyzer. The measurements were carried out under N$_2$ flow (40 ml min^{-1}) by heating from 40 to 800 °C at 10 °C/min. The temperature of maximum degradation rate, T_{max}, has been calculated from the TGA curve derivative as the peak maximum.

WIDE ANGLE X-RAY SCATTERING Wide angle X-ray scattering analysis (WAXS) was carried out at RT with a PANalytical X'Pert PRO diffractometer equipped with an XCelerator detector. Cu anode was used as X-ray source (λ_1 = 0.15406 nm, λ_2 = 0.15443 nm). The degree of crystallinity (χ_c) was

evaluated as the ratio of the crystalline peak areas to the total area under the scattering curve by using the WinFit program.[47]

STRESS-STRAIN MEASURMENTS Tensile testing was performed using an Instron 5966 tensile testing machine equipped with rubber grip and a 500 N load cell controlled by computer. Rectangular films (5×20 mm^2) were employed and 10 mm/min crosshead speed was adopted. Load-displacement values were converted to stress-strain curves. Tensile elastic modulus was determined from the initial linear slope of the curve for seven replicate specimens and the result provided as the average value $\pm$ standard deviation.

COMPOSTING TEST Composting studies have been carried out at 58 °C in compost kindly supplied by HerAmbiente S.p.A. Films of about 30×30 mm^2 were placed in a 100 mL bottle together with the compost (20 g) and 10 mL of deionized water. After different times of incubation, the specimens were withdrawn from the compost, washed and dried under vacuum to constant weight.[48]

The percentage weight loss was calculated as:

$$(mi - mf)/mi \cdot 100$$

where m_f and m_i are the final and the initial sample weight, respectively.

SURFACE CHARACTERIZATION The surface modifications after composting tests have been analyzed by using a desktop Phenom scan electron microscope (SEM). Prior to analysis, the incubated samples were metal sputtered and glued on aluminum holders.

WATER CONTACT ANGLES MEASURMENTS Static contact angle measurements were performed on the films by using a KSV CAM101 instrument (Helsinki, Finland) at room temperature by acquiring the profile images of deionized water drops deposited with a syringe. Several measurements were performed for each film, and water contact angles (WCA) were calculated as the average value $\pm$ standard deviation.

RESULTS AND DISCUSSION

MOLECULAR CHARACTERIZATION

The chemical structure of the synthetized copolymers, with general formula of P(BS$_m$BPripol$_n$), is reported in **Figure 1**. As one can see, the copolymeric backbone is characterized by the presence of BS blocks and BPripol ones. From the chemical point of view, the two segments differ for the acid sub-unit: the succinic moiety being linear and short; the Pripol one being longer and containing an aliphatic six carbons ring together with aliphatic side chains on this latter.
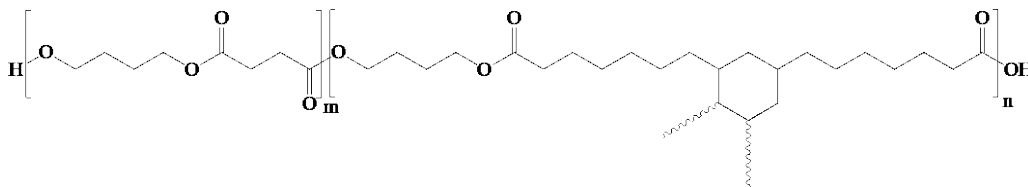

Figure 1. Chemical structure of P(BS$_m$BPripol$_n$) random copolymers (Pripol 1009 cyclohexane side branches length is 7/9 carbon atoms each).

Chemical structure and composition have been determined by ^{1}H-NMR spectroscopy. As an example, **Figure 2a** shows the ^{1}H-NMR spectrum of P(BS$_{60}$BPripol$_{40}$), with the relative peak assignment confirming the chemical structure, and allowing the calculation of the actual composition from the normalized area of the peaks c and f ascribable to the succinic and Pripol moieties, respectively. The molar amount of BS co-units is reported in **Table 1**.

Molecular characterization has been completed by performing ^{13}C-NMR (**Figure 2b**), from which has been possible to calculate the degree of randomness (b), the length (L) and average molar mass (W) of block [86,87]. In particular, the region in between 64.4 and 63.4 ppm (**Figure 2b**, insert), where the butanediol carbon atoms of the –OCH$_2$- group are located, has been used. As one can see, four different signals for the carbons in α-position to the carboxylic oxygen atoms can be detected: the k peak corresponding to S-B-S triads; the o peak due to Pripol-B-Pripol triads; the k_1 and o_1 peaks related to the S-B-Pripol triads. The degree of randomness b has been calculated from the relative intensity of these signals. As well known, b is 1 for random copolymers, equal to 2 for alternate copolymers, is null for a mixture of two homopolymers and 0<b<1 for block copolymers. The degree of randomness (b) was calculated according to the equation:

$$b = P_{S-Pripol} + P_{Pripol-S}$$

where P$_{S-Pripol}$ and P$_{Pripol-S}$ are the probability of finding a S subunit next to a Pripol one and the probability of finding a Pripol moiety followed by a S one, respectively, and can be expressed as follows:

$$P_{S-Pripol} = \frac{I_{k1}}{I_{k1} + I_k}; \qquad P_{Pripol-S} = \frac{I_{o1}}{I_{o1} + I_o}$$

where I_k, I_{k1}, I_{o1}, I_o represent the integrated intensities of the resonance peaks of the S-B-S, S-B-Pripol, Pripol-B-S, Pripol-B-Pripol triads, respectively.

Additionally, the length (L) and average molar mass (W) of the BS and BPripol blocks in the copolymer chain are defined as:

$$L_{BS} = \frac{1}{P_{S-Pripol}}; \qquad L_{BPripol} = \frac{1}{P_{Pripol-S}}$$

$$W_{BS} = \frac{1}{P_{S-Pripol}} * M_{BS}; \qquad W_{BPripol} = \frac{1}{P_{Pripol-S}} * M_{BPripol}$$

where M$_{BS}$ and M$_{BPripol}$ are the molar mass of BS and BPripol repeating units, respectively. The degree of randomness is very close to 1 for all the copolymers (**Table 1**) suggesting the random distribution of co-units. The length and average molar mass of the BS and BPripol blocks (L$_{BS}$, L$_{BPripol}$ and W$_{BS}$, W$_{BPripol}$), reported in **Table 1**, are directly proportional to the molar amount of the succinic and the Pripol subunits contained in the polymer backbone. In **Table 1** are also reported the number molecular weight (M$_n$) and the dispersity (D) determined by GPC analysis. The high M$_n$ values together with D parameter close to 2 suggest a good control during the polymerization process, also confirmed by the random nature of the copolymers under study.

Table 1. Molecular characterization data of PBS and P(BS$_m$BPripol$_n$) copolymers

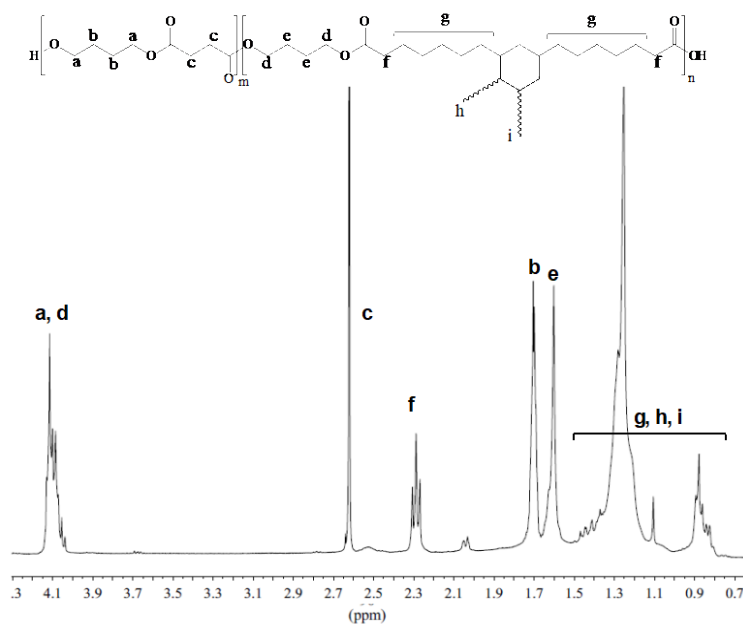| Sample	BS mol% feed	BS mol% ^{1}H-NMR	L_{BS}	$L_{BPripol}$	W_{BS} g/mol	$W_{BPripol}$ g/mol	b	M_n g/mol	D
PBS	100	100	-	-	55000	-	-	55000	2.0
P(BS$_{88}$BPripol$_{12}$)	90	88	8.3	1.2	1428	704	1.02	46000	2.1
P(BS$_{73}$BPripol$_{27}$)	80	73	4.3	1.4	740	896	0.96	46000	2.1
P(BS$_{59}$BPripol$_{41}$)	70	59	2.5	1.6	430	1024	1.03	39000	2.2

Figure 2a. ^{1}H-NMR spectrum of P(BS$_{59}$BPripol$_{41}$) with the relative peak assignment.
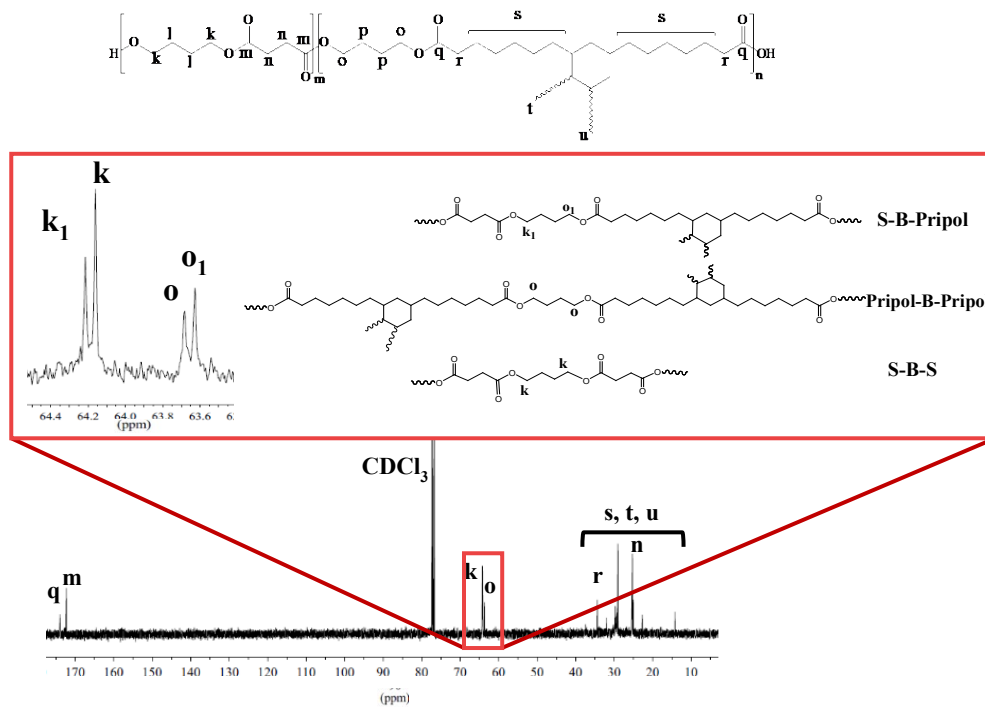
S-B-S

6

Figure 2b. ^{13}C-NMR (bottom) spectrum of P(BS59BPripol41) with the relative peak assignment. Insert: magnification of the 64.6-63.4 ppm region and schematic representation of S-B-Pripol, Pripol-B-Pripol and S-B-S triads.

THERMAL, STRUCTURAL AND SURFACE CHARACTERIZATION

Table 2 reports the thermal (DSC and TGA), structural (WAXS) and surface (WCA) characterization data of the polymer films under investigation.

As concern the thermogravimetric results, **Figure 3** shows the TGA curves, i.e., the gravimetric weight loss the samples undergo during heating in inert atmosphere.
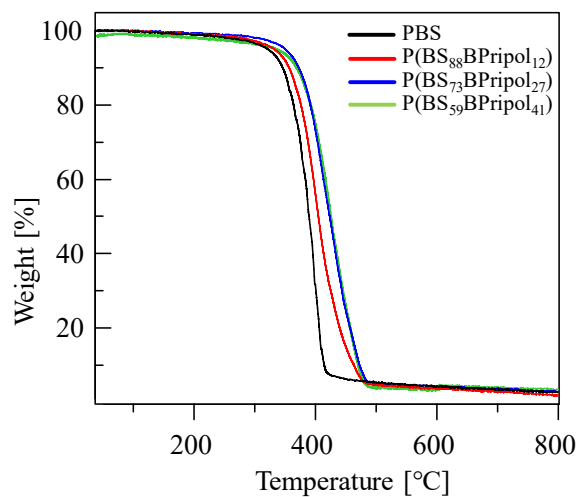

Figure 3. TGA traces of PBS and P(BS$_m$BPripol$_n$) samples obtained by heating at 10°C/min under inert atmosphere.

7

As one can see from the TGA curves (**Figure 3**) and T_{max} values (**Table 2**) the thermal stability, already high for PBS homopolymer, raises in the copolymers as the amount of Pripol 1009 is increased. This effect has been correlated to the decrease of -COOR- per unit length of polymer chain as succinic subunit is replaced by Pripol one. This last, in fact, is mainly composed of methylene groups that are more chemically and thermally stable. The improvement of the thermal resistance is very advantageous in view of the final application and is in line with one of the characteristics claimed for Pripol 1009. The polymers have been also subjected to DSC analysis. The first scan curves of the as obtained films and the second scan after melt quenching are reported in **Figure 4** and the corresponding thermal data are summarized in **Table 2**. As one can see from **Figure 4 left**, all the polymers are semicrystalline, i.e. present at low temperature the endothermic phenomenon associated to the glass to rubber transition and at high temperature the crystal melting peak. As concern the crystal characteristics of each polymer, the calorimetric results show the introduction of Pripol moieties in the PBS macromolecule backbone causes a reduction of both T_m and ΔH_m indicating the formation of a less abundant and at the same time less perfect crystalline phase, as a consequence of the progressive reduction of the crystallization capability of PBS segments which become increasingly shorter as the co-unit content increases, as indicated by the reduction of the average molar mass of the BS blocks, W_{BS}, reported in **Table 1**.
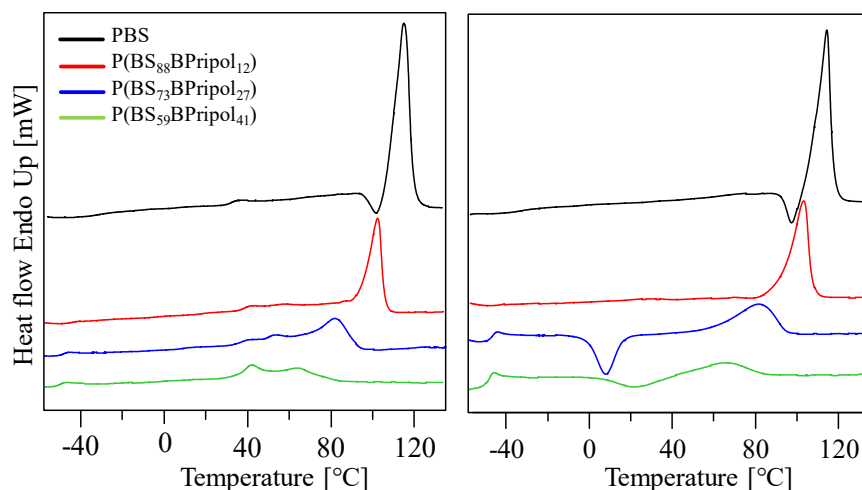

Figure 4. DSC first (left) and second (right) scans of PBS and P(BS$_m$BPripol$_n$) samples. Heating rate: 20 °C/min under nitrogen flow.

The glass transition temperatures, directly related to the amorphous phase mobility, have been evaluated from the second heating scan (**Figure 4 right**). All the samples are in the rubbery state at room temperature being characterized by very low T_g values. The replacement of the short succinic subunit with the very long Pripol ones deeply enhances chain mobility determining an important reduction of T_g from -35 °C for PBS to -51 °C in the case of P(BS$_{59}$BPripol$_{41}$). Simultaneously, there is a decrease in the ability to crystallize. In fact, after melt quenching, PBS homopolymer and P(BS$_{80}$BPripol$_{20}$) copolymer are still able to crystallize during the cooling step presenting just the melting peak in the second scan trace. P(BS$_{70}$BPripol$_{30}$) chains are partially locked in the amorphous state by rapid cooling of the melt and crystallize during the second scan above T_g and melt at higher temperature, nevertheless, being $\Delta H_c < \Delta H_m$, the macromolecules had not been quenched. P(BS$_{59}$BPripol$_{41}$) copolymer shows a similar thermal behavior even if both T_m and ΔH_m are lower. Moreover, for the highest Pripol-containing copolymer, $\Delta H_c = \Delta H_m$, indicating the complete rubbery state of the material after melt quenching.

8

Table 2. Thermal, structural and surface characterization data of PBS and P(BS$_m$BPripol$_n$) copolymers

Sample	DSC								TGA	WAXS	WCA
	First scan		Second scan								
	T_m	ΔH_m	T_g	Δc_p	T_c	ΔH_c	T_m	ΔH_m	T_{max}	χ_c	$^\circ$
	°C	J/g	°C	J/g*°C	°C	J/g	°C	J/g	°C	%	
PBS	114	50	-35	0.192	/	/	114	51	399	46	89±2
P(BS$_{88}$BPripol$_{12}$)	102	44	-42	0.231	/	/	104	44	414	40	100±2
P(BS$_{73}$BPripol$_{27}$)	82	30	-47	0.360	7	20	82	29	424	28	96±2
P(BS$_{59}$BPripol$_{41}$)	42	20	-51	0.413	22	12	65	13	426	22	95±2

The compression molded films have also been studied by wide angle X-ray scattering. WAXS patterns are reported in **Figure 5** while the crystallinity degree, χc, is summarized in **Table 2**. In confirmation of the calorimetric results, all the samples present a diffractogram that, in addition to the amorphous halo coming from the amorphous portion, shows a series of reflections typical of the α-PBS lattice (main reflections at 19.5 and 22.5 2θ). As co-unit content rises, one can observe a progressive increase of the area under the bell shaped background line, directly related to the amorphous phase fraction, accompanied by the reduction of the reflection intensities, due to the ordered phase. This trend determines the decrement of crystallinity degree (**Table 2**) as already evidenced by DSC experiments. The peak position does not change by copolymerization suggesting the complete exclusion of Pripol segments from the α-PBS lattice. Such result is not surprising considering the strong difference in the chemical structure of BS and BPripol co-units.
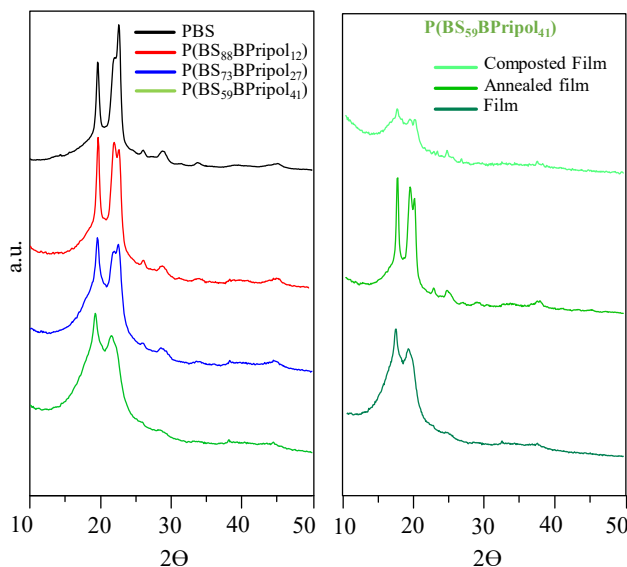
Figure 5. WAXS spectra of: PBS and P(PBS$_m$BPripol$_n$) copolymers films (left); P(PBS$_{59}$BPripol$_{41}$) film incubated in compost for 110 days (right).

The hydrophobic character of the polymer films has been evaluated by water contact angle (WCA) measurements, whose values are reported in **Table 2**. As one can see, the lowering of -COOR- group number per unit length, consequent to the substitution of succinic subunit with Pripol 1009 moieties, produces an increase of the WCA values meaning an enhancement of the surface hydrophobicity. Surprisingly, the effect is more pronounced in the lowest Pripol 1009 containing copolymer, P(BS$_{88}$BPripol$_{12}$), that presents a WCA around 10° higher than that of PBS homopolymer. This result could be related to the crystalline phase portion, higher in P(BS$_{88}$BPripol$_{12}$) than in the other copolymers, producing a decrease in the wettability of the sample surface.[88] Moreover, the development of crystals, exclusively composed of BS sequences, causes an enrichment of the amorphous phase in the more hydrophobic BPripol blocks that determine the WCA value rising.

MECHANICAL PROPERTIES The mechanical behavior was evaluated by tensile tests whose results are reported in Figure 6 and Table 3. As shown in Figure 6, the presence of Pripol sub-unit along the PBS chain led to a pronounced decreasing of the elastic modulus (E) as well as tensile strength (σ_b), directly dependent on the amount of Pripol 1009. Moreover, elongation at break (ε_b) increases till a value of 500% for P(BS$_{59}$PBPripol$_{41}$). This effect can be explained on the basis of the reduction of ordered portion evidenced by calorimetric and diffractometric analyses. It is very interesting to note that both P(BS$_{73}$PBPripol$_{27}$) and P(BS$_{59}$PBPripol$_{41}$) copolymers showed absence of yielding, pointing out a typical thermoplastic elastomer nature. In this view, cyclic tests were also performed on the highest Pripol containing copolymer, P(BS$_{59}$PBPripol$_{41}$), by applying different elongation, 50, 100 and 150% and recording the recovery of the specimen after stopping the stretching.
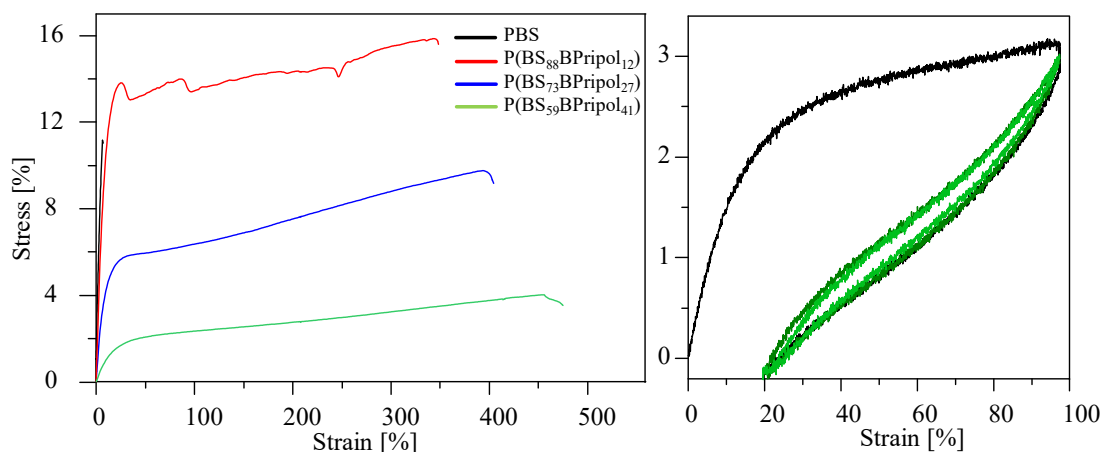

Figure 6. Stress-strain curves of PBS and P(BS$_m$BPripol$_n$) copolymers (left); cyclic mechanical measurement of P(BS$_{59}$BPripol$_{41}$) (right).

Table 3. Mechanical characterization data of PBS and P(BS$_m$BPripol$_n$) copolymers.

Sample	E MPa	σ_y MPa	ε_y %	σ_b MPa	ε_b %
PBS	185±42	/	/	11±2	7±2
P(BS$_{88}$BPripol$_{12}$)	130±40	15±2	22±5	14±1	338±22
P(BS$_{73}$PBPripol$_{27}$)	48±4	/	/	7.8±0.5	392±16
P(BS$_{59}$PBPripol$_{41}$)	14±2	/	/	4.6±0.3	460±22

Table 4. Cyclic mechanical test results for P(BS59BPripol41) copolymer: recovery (r %) and corresponding applied elongation (ε %)

P(BS$_{59}$BPripol$_{41}$)				
ε (%)	50	50*	100	150
r (%)	86±2	86±2*	82±3	60±5

* second measurement on the same specimen after 16 h from the previous test.

Twenty cyclic measurements were carried out for each test. The elastomeric character has been also checked on the same specimen after 16 hours from the previous experiment. The obtained data are collected in **Table 4** while, as an example, in **Figure 6** is reported the mechanical hysteresis loop for 100% elongation. As one can see, P(BS$_{59}$PBPripol$_{41}$) film shows very good recovery capability, till 86% for elongation of 50%, that keeps constant in a second measurement on the same specimen after 16 hours from the previous test. The evidenced behavior is characteristic of block copolymers composed of amorphous rubbery segments, soft blocks responsible for high elongation capability, alternating crystallizable sequences, hard blocks responsible for the elastic return. The copolymers object of this study are characterized by a random distribution of the co-units along the polymer chain as previously discussed, nevertheless, the high molecular mass of Pripol moiety means that the same subunit itself can be considered a block. The length and average molar mass of the BS and BPripol blocks (**Table 1**), are high enough to allow hard blocks (BS) develop crystalline phase (evidenced by DSC and WAXS analyses and responsible for the elastic return), alternating long soft blocks (BPripol) accountable for the outstanding elongation capability. In conclusion, the presence of the biobased Pripol subunit confers to a random copolymer the typical behaviour of a block copolymer.

COMPOSTABILITY Biodegradability of PBS and P(BS$_m$BPripol$_n$) copolymers was tested by compost degradation experiments. The gravimetric weight loss, the copolymer composition and the calorimetric melting temperature and enthalpy values (T$_m$ and ΔH$_m$) were evaluated at different incubation times. The results reported in **Figure 7** have shown a marked weight loss as the incubation time increases, directly proportional to Pripol moieties percentage, also evidenced by the SEM images of the composted film surface (**Figure 7** inserts). A simultaneous variation of composition has also been detected by NMR analysis: as degradation proceeds, the copolymer films are progressively enriched in Pripol content, by 30, 10 and 2% for P(BS$_{88}$BPripol$_{12}$), P(BS$_{73}$BPripol$_{27}$) and P(BS$_{59}$BPripol$_{41}$), respectively, indicating the bacteria present in compost preferentially attack the BS sequences.
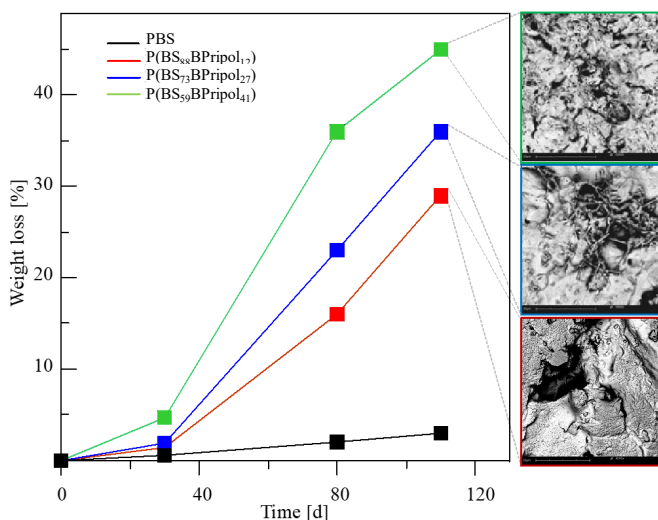

Figure 7. Gravimetric weight loss % vs. time (left) and the SEM images [50x50 μm] after 110 days of compost incubation (right) for PBS and its copolymers.
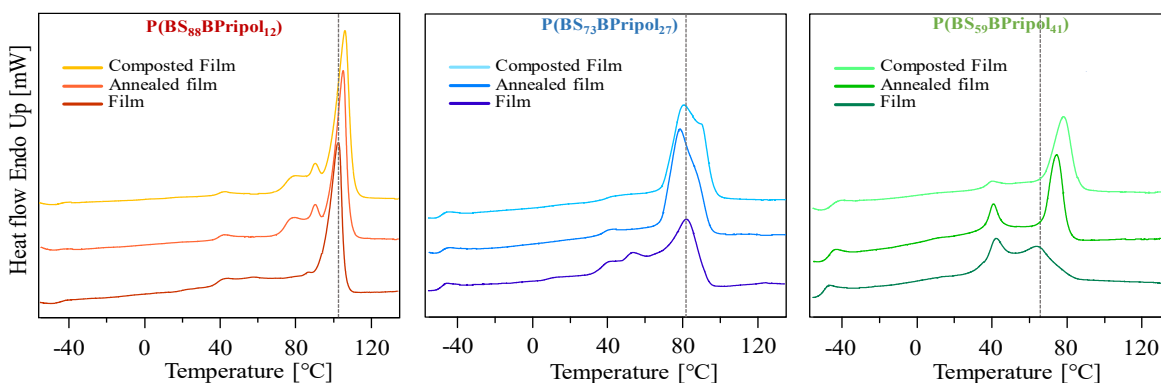
Figure 8. DSC first scan of P(BS$_m$BPripol$_n$) copolymers. From the bottom to the top: neat film; annealed film (58 °C); composted film (110 days). Heating rate: 20 °C/min under nitrogen flow.

This result may surprise at first sight since BS segments are less mobile (higher T$_g$) and, moreover, are partially locked in crystal lattices that are commonly less prone to be degraded with respect to the amorphous portion. The reason for the slower composting process for BPripol segments can be found in the lower density of -COOR- functional groups in the copolymers with respect to PBS homopolymer. This result is particularly interesting taking into account that in most of PBS-based copolymers the co-unit is the fastest degrading moiety. The preferential degradation of BS segments is also corroborated by the reduction of crystalline phase, exclusively composed of BS sequences, evidenced by DSC analysis. In **Figure 8** are reported the calorimetric traces of the copolymer films incubated in compost for 110 days together with the neat films and the films annealed at the composting temperature (58 °C) but in absence of compost. The annealed samples have been considered to evaluate the effect of the composting temperature separately from the bacteria degradation. As one can see, the thermal annealing itself produces a reorganization of the crystalline phase that melts at higher temperature with respect to the as prepared compression molded films. As concern the degraded copolymer films, it is interesting to note a further increase of T$_m$ together with a reduction of the endotherm underlying area (ΔH$_m$), directly related to a reduction of the low melting BS crystals. The reduction of crystalline phase has also been detected by WAXS analysis. As an example, in **Figure 5 right** are collected the diffractograms of P(PBS$_{59}$BPripol$_{41}$) film incubated for 110 days, the and the annealed material.

CONCLUSIONS 100% biobased random copolymers of PBS containing Pripol 1009 moieties were successfully synthesized through a green solvent-free simple process, which can be easily scale-up at industrial level.

The introduction of Pripol moieties significantly improved PBS thermal stability and flexibility, as proved by TGA analysis and mechanical response, respectively. A significant reduction of elastic modulus and a parallel increase of elongation at break with Pripol content was indeed observed, the copolymer with the highest Pripol amount showing the mechanical behavior typical of a thermoplastic elastomer characterized by a good elastic recovery despite its random nature.

PBS biodegradation in compost was significantly increased thanks to Pripol subunits and, interestingly, BS sequences appeared to be those preferentially attacked by the microorganisms though their semicrystalline nature.

In conclusion, copolymer composition revealed to be a very efficient tool to tune final material properties, permitting in case of high Pripol content to obtain a highly stable, thermoplastic elastomer and fast degrading material, potentially exploitable for soft tissue engineering as well for sustainable flexible packaging, fields where PBS homopolymer cannot be exploitable because of its too high stiffness.

References.

(1)   Ryu, H.W; Kang K.H; Yun, J.S. Bioconversion of Fumarate to Succinicate Using Glycerol as a Carbon Source. *Appl. Biochem. Biotechnol.* **1999**, *78*, 511–520.

(2)   Delhomme, C.; Weuster-Botz, D.; Kühn, F. E. Succinic Acid from Renewable Resources as a C4 Building-Block Chemical - A Review of the Catalytic Possibilities in Aqueous Media. *Green Chem.* **2009**, *11* (1), 13–26. https://doi.org/10.1039/b810684c.

(3)   Bechthold, I.; Bretz, K.; Kabasci, S.; Kopitzky, R.; Springer, A. Succinic Acid: A New Platform Chemical for Biobased Polymers from Renewable Resources. *Chem. Eng. Technol.* **2008**, *31* (5), 647–654. https://doi.org/10.1002/ceat.200800063.

(4)   Kohli, K.; Prajapati, R.; Sharma, B. K. Bio-Based Chemicals from Renewable Biomass for Integrated Biorefineries. *Energies* **2019**, *12* (2). https://doi.org/10.3390/en12020233.

(5)   Gunnarsson, I. B.; Kuglarz, M.; Karakashev, D.; Angelidaki, I. Thermochemical Pretreatments for Enhancing Succinic Acid Production from Industrial Hemp (Cannabis Sativa L.). *Bioresour. Technol.* **2015**, *182*, 58–66. https://doi.org/10.1016/j.biortech.2015.01.126.

(6)   Efsa. *Call for Food Additives Usage Level and / or Concentration Data in Food and Beverages in-Tended for Human Consumption*; **2013**.

(7)   De Barros, M.; Freitas, S.; Padilha, G. S.; Alegre, R. M. Biotechnological Production of Succinic Acid by Actinobacillus Succinogenes Using Different Substrate. *Chem. Eng. Trans.* **2013**, *32* (April 2019), 985–990. https://doi.org/10.3303/CET1332165.

(8)   Yim, H.; Haselbeck, R.; Niu, W.; Pujol-Baxley, C.; Burgard, A.; Boldt, J.; Khandurina, J.; Trawick, J.D.; Osterhout, O.E.; Stephen, R.; Estadilla, J.; Teisan, S.; Schreyer H.B.; Andrae, S.; Yang, T.H.; Lee, S.Y. Metabolic Engineering of Escherichia Coli for Direct Production of 1,4-Butanediol. *Nat. Chem. Biol.* **2011**, *7*, 445–452.

(9)   Burgard, A.; Burk, M. J.; Osterhout, R.; Van Dien, S.; Yim, H. Development of a Commercial Scale Process for Production of 1,4-Butanediol from Sugar. *Curr. Opin. Biotechnol.* **2016**, *42*, 118–125. https://doi.org/10.1016/j.copbio.2016.04.016.

(10)   Cok, B.; Tsiropoulos, I.; Succinic Acid Production Derived from Carbohydrates: An Energy and Greenhouse Gas Assessment of a Platform Chemical toward a Bio-Based Economy. *BIOFUEL BIOPROD BIOR* **2014**, *8* (1), 16–29. https://doi.org/10.1002/bbb.

(11)   Xu, J. *Microbial Succinic Acid, Its Polymer Poly(Butylene Succinate), and Applications*; Chen GQ, Ed.; Springer Berlin Heidelberg: Berlin, **2010**.

(12)   Habib Ullah, M.; Mahadi, W. N. L.; Latef, T. A. Aerogel Poly(Butylene Succinate) Biomaterial Substrate for RF and Microwave Applications. *Sci. Rep.* **2015**, *5*, 1–8. https://doi.org/10.1038/srep12868.

(13)   Chen, Z.; Hu, J.; Ju, J.; Kuang, T. Fabrication of Poly(Butylene Succinate)/Carbon Black Nanocomposite Foams with Good Electrical Conductivity and High Strength by a Supercritical CO2 Foaming Process. *Polymers (Basel).* **2019**, *11* (11). https://doi.org/10.3390/polym11111852.

(14)   Lin, C. S.; Shih, Y. F.; Jeng, R. J.; Dai, S. A.; Lin, J. J.; Lee, C. C. Nanocomposites with Enhanced Electrical Properties Based on Biodegradable Poly(Butylene Succinate) and Polyetheramine Modified Carbon Nanotube. *J. Taiwan Inst. Chem. Eng.* **2012**, *43* (2), 322–328. https://doi.org/10.1016/j.jtice.2011.10.009.

(15) Wattanawong, N.; Chatchaipaiboon, K.; Sreekirin, N.; Aht-Ong, D. Migration, Physical and Antibacterial Properties of Silver Zeolite/Poly(Butylene Succinate) Composite Films for Food Packaging Applications. *J. Reinf. Plast. Compos.* **2020**, *39* (3–4), 95–110. https://doi.org/10.1177/0731684419893440.

(16) Sapuan, S. M., Nazrin, A., Ilyas, R. A., Sherwani, S. F. K., & Syafiq, R. Nanocellulose Reinforced Thermoplastic Starch (TPS), Poly (Lactic) Acid (PLA), and Poly (Butylene Succinate)(PBS) for Food Pack-Aging Applications. *Front. Chem.* **2020**, *8*.

(17) Cornish, K.; Vodovotz, Y.; Accepted, J. NARROWING THE GAP FOR BIOPLASTIC USE IN FOOD PACKAGING - AN UPDATE. **2020**. https://doi.org/10.1021/acs.est.9b03755.

(18) Hongsriphan, N.; Pinpueng, A. Properties of Agricultural Films Prepared from Biodegradable Poly(Butylene Succinate) Adding Natural Sorbent and Fertilizer. *J. Polym. Environ.* **2019**, *27* (2), 434–443. https://doi.org/10.1007/s10924-018-1358-5.

(19) Ayu, R. S.; Khalina, A.; Harmaen, A. S.; Zaman, K.; Mohd Nurrazi, N.; Isma, T.; Lee, C. H. Effect of Empty Fruit Brunch Reinforcement in PolyButylene-Succinate/Modified Tapioca Starch Blend for Agricultural Mulch Films. *Sci. Rep.* **2020**, *10* (1), 1–7. https://doi.org/10.1038/s41598-020-58278-y.

(20) Venkatesan, R.; Rajeswari, N. Preparation, Mechanical and Antimicrobial Properties of SiO 2/ Poly(Butylene Adipate-Co-Terephthalate) Films for Active Food Packaging. *Silicon* **2019**, *11* (5), 2233–2239. https://doi.org/10.1007/s12633-015-9402-8.

(21) Hassan, E. A. M.; Elarabi, S. E.; Wei, Y.; Yu, M. Biodegradable Poly (Lactic Acid)/Poly (Butylene Succinate) Fibers with High Elongation for Health Care Products. *Text. Res. J.* **2018**, *88* (15), 1735–1744. https://doi.org/10.1177/0040517517708538.

(22) Zia, K. M.; Noreen, A.; Zuber, M.; Tabasum, S.; Mujahid, M. Recent Developments and Future Prospects on Bio-Based Polyesters Derived from Renewable Resources: A Review. *Int. J. Biol. Macromol.* **2016**, *82*, 1028–1040. https://doi.org/10.1016/j.ijbiomac.2015.10.040.

(23) Rameshkumar, S.; Shaiju, P.; Connor, K. E. O.; P, R. B. Bio-Based and Biodegradable Polymers - State-of-the-Art, Challenges and Emerging Trends. *Curr. Opin. Green Sustain. Chem.* **2019**. https://doi.org/10.1016/j.cogsc.2019.12.005.

(24) Shen, S.; Rodion, K.; Sengül, T. Polylactide (PLA) and Its Blends with Poly(Butylene Succinate) (PBS): A Brief Review. *Polymers (Basel).* **2019**, 1–21.

(25) Helanto, K.; Matikainen, L.; Talja, R.; Rojas, O. J. Bio-Based Polymers for Sustainable Packaging and Biobarriers: A Critical Review. **2019**, *14* (Greene 2014), 4902–4951.

(26) Gumede, T. P.; Luyt, A. S.; Müller, A. J. Review on PCL , PBS , and PCL / PBS Blends Containing Carbon Nanotubes. **2018**, *12* (6), 505–529.

(27) Azim, H.; Dekhterman, A.; Jiang, Z.; Gross, R. A. Candida Antarctica Lipase B Catalyzed Synthesis of Poly(Butylene Succinate): Shorter Chain Building Blocks Also Work. *ACS Symp. Ser.* **2008**, *999*, 285–293. https://doi.org/10.1021/bm060574h.

(28) Xu, J.; Guo, B. H. Poly(Butylene Succinate) and Its Copolymers: Research, Development and Industrialization. *Biotechnol. J.* **2010**, *5* (11), 1149–1163. https://doi.org/10.1002/biot.201000136.

(29) Ojansivu, M.; Johansson, L.; Vanhatupa, S.; Tamminen, I.; Hannula, M.; Hyttinen, J.; Kellomäki, M.; Miettinen, S. Knitted 3D Scaffolds of Polybutylene Succinate Support Human Mesenchymal

Stem Cell Growth and Osteogenesis. **2018**, *2018*.

(30) Huang, A.; Peng, X.; Geng, L.; Zhang, L.; Huang, K.; Chen, B. Electrospun Poly(Butylene Succinate)/Cellulose Nanocrystals Bio- Nanocomposite Scaffolds for Tissue Engineering: Preparation, Characterization and in Vitro Evaluation. *Polym. Test.* **2018**, *71* (July), 101–109. https://doi.org/10.1016/j.polymertesting.2018.08.027.

(31) Domínguez-Robles, J.; Larrañeta, E.; Fong, M. L.; Martin, N. K.; Irwin, N. J.; Mutjé, P.; Tarrés, Q.; Delgado-Aguilar, M. Lignin/Poly(Butylene Succinate) Composites with Antioxidant and Antibacterial Properties for Potential Biomedical Applications. *Int. J. Biol. Macromol.* **2020**, *145*, 92–99. https://doi.org/10.1016/j.ijbiomac.2019.12.146.

(32) Pajoumshariati, S.; Shirali, H.; Yavari, S. K.; Sheikholeslami, S. N.; Lotfi, G.; Mashhadi Abbas, F.; Abbaspourrad, A. GBR Membrane of Novel Poly (Butylene Succinate-Co-Glycolate) Co-Polyester Co-Polymer for Periodontal Application. *Sci. Rep.* **2018**, *8* (1), 1–16. https://doi.org/10.1038/s41598-018-25952-1.

(33) Chen, L.; Cheng, H. H.; Xiong, J.; Zhu, Y. T.; Zhang, H. P.; Xiong, X.; Liu, Y. M.; Yu, J.; Guo, Z. X. Improved Mechanical Properties of Poly(Butylene Succinate) Membrane by Co-Electrospinning with Gelatin. *Chinese J. Polym. Sci. (English Ed.* **2018**, *36* (9), 1063–1069. https://doi.org/10.1007/s10118-018-2112-0.

(34) Kang, Y. G.; Wei, J.; Kim, J. E.; Wu, Y. R.; Lee, E. J.; Su, J.; Shin, J. W. Characterization and Osteogenic Evaluation of Mesoporous Magnesium-Calcium Silicate/Polycaprolactone/Polybutylene Succinate Composite Scaffolds Fabricated by Rapid Prototyping. *RSC Adv.* **2018**, *8* (59), 33882–33892. https://doi.org/10.1039/C8RA06281A.

(35) Tang, X.; Dai, J.; Sun, H.; Nabanita, S.; Petr, S.; Tang, L.; Cheng, Q.; Wang, D.; Wei, J. Copper-Doped Nano Laponite Coating on Poly(Butylene Succinate) Scaffold with Antibacterial Properties and Cytocompatibility for Biomedical Application. *J. Nanomater.* **2018**, *2018*. https://doi.org/10.1155/2018/5470814.

(36) Gigli, M.; Fabbri, M.; Lotti, N.; Gamberini, R.; Rimini, B.; Munari, A. Poly(Butylene Succinate)-Based Polyesters for Biomedical Applications: A Review in Memory of Our Beloved Colleague and Friend Dr. Lara Finelli. *Eur. Polym. J.* **2016**, *75*, 431–460. https://doi.org/10.1016/j.eurpolymj.2016.01.016.

(37) Moraes, R.S.; Ricardo, N.; Saez, V. Synthesis of Magnetic Composite of Poly(Butylene Succinate) and Magnetite for the Controlled Release of Meloxicam. **2018**, *2* (1), 2–5. https://doi.org/10.15406/mojps.2018.02.00044.

(38) Zhao, Y.; Guo, W.; Lu, Q.; Zhang, S. Preparation of Poly(Butylene Succinate)-Poly[2-(Dimethylamino)Ethyl Methacrylate] Copolymers and Their Applications as Carriers for Drug Delivery. *Polym Int.* **2018***, 67, 708–716. https://doi.org/10.1002/pi.5559.

(39) Gigli, M.; Lotti, N.; Gazzano, M.; Siracusa, V.; Finelli, L.; Munari, A.; Rosa, M. D. Biodegradable Aliphatic Copolyesters Containing PEG-like Sequences for Sustainable Food Packaging Applications. *Polym. Degrad. Stab.* **2014**, *105* (1), 96–106. https://doi.org/10.1016/j.polymdegradstab.2014.04.006.

(40) Shi, M.; Cheng, T.; Zou, H.; Zhang, N.; Huang, J.; Xian, M. The Preparation and Biomedical Application of Biopolyesters. *Mini Rev. Med. Chem.* **2019**. https://doi.org/10.2174/1389557519666191015211156.

(41)   Xiaonan, L.; Gang, L.; Qin, S. Structure and Properties of Nano-Hydroxyapatite/Poly(Butylene Succinate) Porous Scaffold for Bone Tissue Engineering Prepared by Using Ethanol as Porogen. *J. Biomater. Appl.* **2018**, *33* (6), 776–791.

(42)   Cristofaro, F.; Gigli, M.; Bloise, N.; Chen, H.; Bruni, G.; Munari, A.; Moroni, L.; Lotti, N.; Visai, L. Influence of the Nanofiber Chemistry and Orientation of Biodegradable Poly(Butylene Succinate)-Based Scaffolds on Osteoblast Differentiation for Bone Tissue Regeneration. *Nanoscale* **2018**, *10* (18), 8689–8703. https://doi.org/10.1039/c8nr00677f.

(43)   Chen, H.; Gigli, M.; Gualandi, C.; Truckenmüller, R.; van Blitterswijk, C.; Lotti, N.; Munari, A.; Focarete, M. L.; Moroni, L. Tailoring Chemical and Physical Properties of Fibrous Scaffolds from Block Copolyesters Containing Ether and Thio-Ether Linkages for Skeletal Differentiation of Human Mesenchymal Stromal Cells. *Biomaterials* **2016**, *76*, 261–272. https://doi.org/10.1016/j.biomaterials.2015.10.071.

(44)   Fabbri, M.; Gigli, M.; Costa, M.; Govoni, M.; Seri, P.; Lotti, N.; Giordano, E.; Munari, A.; Gamberini, R.; Rimini, B.; et al. The Effect of Plasma Surface Modification on the Biodegradation Rate and Biocompatibility of a Poly(Butylene Succinate)-Based Copolymer. *Polym. Degrad. Stab.* **2015**, *121*, 271–279. https://doi.org/10.1016/j.polymdegradstab.2015.09.015.

(45)   M. Gigli, N. Lotti, M. Gazzano, L. F. and A. M. Synthesis and Characterization of Novel Poly(Butylenesuccinate)-Based Copolyesters Designed as Potential Candidates for Soft Tissue Engineering. *POLYM ENG SCI.,* **2013**, *53*, 491–501. https://doi.org/10.1002/pen.

(46)   Gualandi, C.; Soccio, M.; Saino, E.; Focarete, M. L.; Lotti, N.; Munari, A.; Moroni, L.; Visai, L. Easily Synthesized Novel Biodegradable Copolyesters with Adjustable Properties for Biomedical Applications. *Soft Matter* **2012**, *8* (20), 5466–5476. https://doi.org/10.1039/c2sm25308a.

(47)   Mangaraj, S.; Yadav, A.; Bal, L.M. Application of Biodegradable Polymers in Food Packaging Industry: A Comprehensive Review. *J. Packag. Technol. Res.* **2019**, *3*, 77–96.

(48)   Meena, P. L.; Goel, A.; Rai, V.; S, E. R. Packaging Material and Need of Biodegradable Polymers : A Review. **2017**, *3* (7), 886–896.

(49)   Siracusa, V.; Rosa, M. D. *Sustainable Packaging*; Elsevier Inc., 2018. https://doi.org/10.1016/B978-0-12-811935-8.00008-1.

(50)   Vytejčková, S.; Vápenka, L.; Hradecký, J.; Dobiáš, J.; Hajšlová, J.; Loriot, C.; Vannini, L.; Poustka, J. Testing of Polybutylene Succinate Based Films for Poultry Meat Packaging. *Polym. Test.* **2017**, *60*, 357–364. https://doi.org/10.1016/j.polymertesting.2017.04.018.

(51)   Guidotti, G.; Soccio, M.; Siracusa, V.; Gazzano, M.; Salatelli, E.; Munari, A.; Lotti, N. Novel Random PBS-Based Copolymers Containing Aliphatic Side Chains for Sustainable Flexible Food Packaging. *Polymers (Basel).* **2017**, *9* (12), 1–16. https://doi.org/10.3390/polym9120724.

(52)   Genovese, L.; Lotti, N.; Gazzano, M.; Siracusa, V.; Dalla Rosa, M.; Munari, A. Novel Biodegradable Aliphatic Copolyesters Based on Poly(Butylene Succinate) Containing Thioether-Linkages for Sustainable Food Packaging Applications. *Polym. Degrad. Stab.* **2016**, *132*, 191–201. https://doi.org/10.1016/j.polymdegradstab.2016.02.022.

(53)   Siracusa, V.; Lotti, N.; Munari, A.; Dalla Rosa, M. Poly(Butylene Succinate) and Poly(Butylene Succinate-Co-Adipate) for Food Packaging Applications: Gas Barrier Properties after Stressed Treatments. *Polym. Degrad. Stab.* **2015**, *119*, 35–45. https://doi.org/10.1016/j.polymdegradstab.2015.04.026.

(54) Fortunati, E.; Gigli, M.; Luzi, F.; Dominici, F.; Lotti, N.; Gazzano, M.; Cano, A.; Chiralt, A.; Munari, A.; Kenny, J. M.; et al. Processing and Characterization of Nanocomposite Based on Poly(Butylene/Triethylene Succinate) Copolymers and Cellulose Nanocrystals. *Carbohydr. Polym.* **2017**, *165*, 51–60. https://doi.org/10.1016/j.carbpol.2017.02.024.

(55) Gigante, V.; Coltelli, M.; Vannozzi, A.; Panariello, L.; Fusco, A.; Trombi, L.; Donnarumma, G. Flat Die Extruded Biocompatible Poly(Lactic Acid)/Poly(Butylene Succinate) (PBS) Based Films. *Polymers* **2019**, 11, 1857. doi:10.3390/polym11111857

(56) Petchwattana, N.; Covavisaruch, S.; Wibooranawong, S.; Naknaen, P. Antimicrobial Food Packaging Prepared from Poly(Butylene Succinate) and Zinc Oxide. *Meas. J. Int. Meas. Confed.* **2016**, *93*, 442–448. https://doi.org/10.1016/j.measurement.2016.07.048.

(57) Finelli, L.; Fiorini, M.; Siracusa, V.; Lotti, N.; Munari, A. Synthesis and Characterization of Poly (Ethylene Isophthalate-Co-Ethylene Terephthalate) Copolyesters. *J. App. Polym. Sci.* **2003**, *92* **(**1), 186-193.

(58) Zheng, L.; Li, C.; Zhang, D.; Guan, G.; Xiao, Y.; Wang, D. Multiblock Copolymers Composed of Poly(Butylene Succinate) and Poly(1,2-Propylene Succinate): Effect of Molar Ratio of Diisocyanate to Polyester-Diols on Crosslink Densities, Thermal Properties, Mechanical Properties and Biodegradability. *Polym. Degrad. Stab.* **2010**, *95* (9), 1743–1750. https://doi.org/10.1016/j.polymdegradstab.2010.05.016.

(59) Zheng, L.; Li, C.; Huang, W.; Huang, X.; Zhang, D.; Guan, G.; Xiao, Y.; Wang, D. Synthesis of High-Impact Biodegradable Multiblock Copolymers Comprising of Poly(Butylene Succinate) and Poly(1,2-Propylene Succinate) with Hexamethylene Diisocyanate as Chain Extender. *Polym. Adv. Technol.* **2011**, *22* (2), 279–285. https://doi.org/10.1002/pat.1530.

(60) Mochizuki, M.; Mukai, K.; Yamada, K.; Ichise, N.; Murase, S.; Iwaya, Y. Structural Effects upon Enzymatic Hydrolysis of Poly(Butylene Succinate-Co-Ethylene Succinate)S. *Macromolecules* **1997**, *30* (24), 7403–7407. https://doi.org/10.1021/ma970036k.

(61) Gan, Z.; Abe, H.; Doi, Y. Crystallization, Melting, and Enzymatic Degradation of Biodegradable Poly(Butylene Succinate-Co-Ethylene Succinate) Copolyester. *Biomacromolecules* **2001**, *2* (1), 313–321. https://doi.org/10.1021/bm0056557.

(62) Papageorgiou, G. Z.; Bikiaris, D. N. Synthesis, Cocrystallization, and Enzymatic Degradation of Novel Poly(Butylene-Co-Propylene Succinate) Copolymers. *Biomacromolecules* **2007**, *8* (8), 2437–2449. https://doi.org/10.1021/bm0703113.

(63) Lee, S. H.; Kim, M. N. Isolation of Bacteria Degrading Poly(Butylene Succinate-Co-Butylene Adipate) and Their Lip A Gene. *Int. Biodeterior. Biodegrad.* **2010**, *64* (3), 184–190. https://doi.org/10.1016/j.ibiod.2010.01.002.

(64) Ding, M.; Zhang, M.; Yang, J.; Qiu, J. H. Study on the Enzymatic Degradation of Aliphatic Polyester–PBS and Its Copolymers. *J. Appl. Polym. Sci* **2012**, *124*, 2902–2907.

(65) Gigli, M.; Negroni, A.; Zanaroli, G.; Lotti, N.; Fava, F.; Munari, A. Environmentally Friendly PBS-Based Copolyesters Containing PEG-like Subunit: Effect of Block Length on Solid-State Properties and Enzymatic Degradation. *React. Funct. Polym.* **2013**, *73* (5), 764–771. https://doi.org/10.1016/j.reactfunctpolym.2013.03.007.

(66) Gigli, M.; Negroni, A.; Soccio, M.; Zanaroli, G.; Lotti, N.; Fava, F.; Munari, A. Enzymatic Hydrolysis Studies on Novel Eco-Friendly Aliphatic Thiocopolyesters. *Polym. Degrad. Stab.* **2013**,

98 (5), 934–942. https://doi.org/10.1016/j.polymdegradstab.2013.02.019.

(67) Gigli, M.; Negroni, A.; Soccio, M.; Zanaroli, G.; Lotti, N.; Fava, F.; Munari, A. Influence of Chemical and Architectural Modifications on the Enzymatic Hydrolysis of Poly(Butylene Succinate). *Green Chem.* **2012**, *14* (10), 2885–2893. https://doi.org/10.1039/c2gc35876j.

(68) Fabbri, M.; Guidotti, G.; Soccio, M.; Lotti, N.; Govoni, M.; Giordano, E.; Gazzano, M.; Gamberini, R.; Rimini, B.; Munari, A. Novel Biocompatible PBS-Based Random Copolymers Containing PEG-like Sequences for Biomedical Applications: From Drug Delivery to Tissue Engineering. *Polym. Degrad. Stab.* **2018**, *153*, 53–62. https://doi.org/10.1016/j.polymdegradstab.2018.04.011.

(69) Jeffrey Kuo, C. F.; Wang, H. Y.; Prasannan, A.; Lai, J. Y.; Wang, J. S.; Chang, H. M.; Tsai, H. C. In Vivo Degradation Study of Polyvinylidene Fluoride/Polybutylene Succinate/Modified Organic Montmorillonite Nanocomposite Films Implanted in the Gastrointestinal Tract. *Polym. Degrad. Stab.* **2020**, *172*. https://doi.org/10.1016/j.polymdegradstab.2019.109058.

(70) Nofar, M.; Oguz, H.; Ovalı, D. Effects of the Matrix Crystallinity, Dispersed Phase, and Processing Type on the Morphological, Thermal, and Mechanical Properties of Polylactide-Based Binary Blends with Poly[(Butylene Adipate)-Co-Terephthalate] and Poly[(Butylene Succinate)-Co-Adipate]. *J. Appl. Polym. Sci.* **2019**, *136* (23), 1–11. https://doi.org/10.1002/app.47636.

(71) Xue, B.; He, H. Z.; Huang, Z. X.; Zhu, Z.; Xue, F.; Liu, S.; Liu, B. Fabrication of Super-Tough Ternary Blends by Melt Compounding of Poly(Lactic Acid) with Poly(Butylene Succinate) and Ethylene-Methyl Acrylate-Glycidyl Methacrylate. *Compos. Part B Eng.* **2019**, *172* (December 2018), 743–749. https://doi.org/10.1016/j.compositesb.2019.05.098.

(72) Delamarche, E.; Mattlet, A.; Livi, S.; Gérard, J.-F.; Bayard, R.; Massardier, V. Tailoring Biodegradability of Poly(Butylene Succinate)/Poly(Lactic Acid) Blends With a Deep Eutectic Solvent. *Front. Mater.* **2020**, *7* (February), 1–13. https://doi.org/10.3389/fmats.2020.00007.

(73) Faibunchan, P.; Pichaiyut, S.; Kummerlöwe, C.; Vennemann, N.; Nakason, C. Green Biodegradable Thermoplastic Natural Rubber Based on Epoxidized Natural Rubber and Poly(Butylene Succinate) Blends: Influence of Blend Proportions. *J. Polym. Environ.* **2020**, *28* (3), 1050–1067. https://doi.org/10.1007/s10924-020-01655-5.

(74) Techniques, F.; Lin, S.; Wang, H.; Wang, J.; Wu, T. Enzymatic Degradation of Acrylic Acid-Grafted. **2020**.

(75) Sonseca, A.; Sahay, R.; Stepien, K.; Bukala, J.; Wcislek, A.; McClain, A.; Sobolewski, P.; Sui, X. M.; Puskas, J. E.; Kohn, J.; et al. Architectured Helically Coiled Scaffolds from Elastomeric Poly(Butylene Succinate) (PBS) Copolyester via Wet Electrospinning. *Mater. Sci. Eng. C* **2020**, *108* (September 2019), 110505. https://doi.org/10.1016/j.msec.2019.110505.

(76) Śmigiel-Gac, N.; Pamuła, E.; Krok-Borkowicz, M.; Smola-Dmochowska, A.; Dobrzyński, P. Synthesis and Properties of Bioresorbable Block Copolymers of L-Lactide, Glycolide, Butyl Succinate and Butyl Citrate. *Polymers (Basel).* **2020**, *12* (1). https://doi.org/10.3390/polym12010213.

(77) Bi, T.; Qiu, Z. Synthesis, Thermal and Mechanical Properties of Fully Biobased Poly(Butylene-Co-Propylene 2,5-Furandicarboxylate) Copolyesters with Low Contents of Propylene 2,5-Furandicarboxylate Units. *Polymer (Guildf).* **2020**, *186* (November 2019), 122053. https://doi.org/10.1016/j.polymer.2019.122053.

(78) Ju, J.; Gu, Z.; Liu, X.; Zhang, S.; Peng, X.; Kuang, T. Fabrication of Bimodal Open-Porous Poly

(Butylene Succinate)/Cellulose Nanocrystals Composite Scaffolds for Tissue Engineering Application. *Int. J. Biol. Macromol.* **2020**, *147*, 1164–1173. https://doi.org/10.1016/j.ijbiomac.2019.10.085.

(79) Qi, W.; Taherzadeh, M. J.; Ruan, Y.; Deng, Y.; Chen, J. S.; Lu, H. F.; Xu, X. Y. Denitrification Performance and Microbial Communities of Solid-Phase Denitrifying Reactors Using Poly (Butylene Succinate)/Bamboo Powder Composite. *Bioresour. Technol.* **2020**, *305* (February), 123033. https://doi.org/10.1016/j.biortech.2020.123033.

(80) Zhou, H.; Qu, Z.; Yin, D.; Ye, H.; Yu, K.; Wang, X. A Facile and Green Approach Toward Preparation of Nanocellular Poly(Butylene Succinate)/Hydroxyl-Functionalized Graphene Composite Foam Induced by Nonisothermal Crystallization. *J. Vinyl Addit. Technol.* **2020**, 1–14. https://doi.org/10.1002/vnl.21761.

(81) Nanni, A.; Messori, M. Thermo-Mechanical Properties and Creep Modelling of Wine Lees Filled Polyamide 11 (PA11) and Polybutylene Succinate (PBS) Bio-Composites. *Compos. Sci. Technol.* **2020**, *188* (September 2019), 107974. https://doi.org/10.1016/j.compscitech.2019.107974.

(82) Platnieks, O.; Gaidukovs, S.; Barkane, A.; Gaidukova, G.; Grase, L.; Thakur, V. K.; Filipova, I.; Fridrihsone, V.; Skute, M.; Laka, M. Highly Loaded Cellulose/Poly (Butylene Succinate) Sustainable Composites for Woody-like Advanced Materials Application. *Molecules* **2020**, *25* (1). https://doi.org/10.3390/molecules25010121.

(83) Soccio, M.; Lotti, N.; Finelli, L.; Gazzano, M.; Munari, A. Influence of Transesterification Reactions on the Miscibility and Thermal Properties of Poly(Butylene/Diethylene Succinate) Copolymers. *Eur. Polym. J.* **2008**, *44* (6), 1722–1732. https://doi.org/10.1016/j.eurpolymj.2008.03.022.

(84) Fabbri, M.; Gigli, M.; Gamberini, R.; Lotti, N.; Gazzano, M.; Rimini, B.; Munari, A. Hydrolysable PBS-Based Poly(Ester Urethane)s Thermoplastic Elastomers. *Polym. Degrad. Stab.* **2014**, *108*, 223–231. https://doi.org/10.1016/j.polymdegradstab.2014.03.033.

(85) Soccio M., Lotti N., Gigli M., Finelli L., Gazzano M., M. A. Reactive Blending of Poly(Butylene Succinate) and Poly(Triethylene Succinate): Characterization of the Copolymers Obtained. *Polym. Int.* **2012**, *63*, 1163.

(86) Soccio, M.; Lotti, N.; Gazzano, M.; Govoni, M.; Giordano, E.; Munari, A. Molecular Architecture and Solid-State Properties of Novel Biocompatible PBS-Based Copolyesters Containing Sulphur Atoms. *React. Funct. Polym.* **2012**, *72* (11), 856–867. https://doi.org/10.1016/j.reactfunctpolym.2012.08.002.

(87) Chen, M. S.; Chang, S. J.; Chang, R. S.; Kuo, W. F.; Tsai, H. B. Copolyesters. I. Sequence Distribution of Poly(Butylene Terephthalate-Co-Adipate) Copolyesters Determined by 400 MHz NMR. *J. Appl. Polym.* **1990**, *40*, 1053–1057.

(88) Areias, A. C.; Ribeiro, C.; Sencadas, V.; Garcia-Giralt, N.; Diez-Perez, A.; Gómez Ribelles, J. L.; Lanceros-Méndez, S. Influence of Crystallinity and Fiber Orientation on Hydrophobicity and Biological Response of Poly(l-Lactide) Electrospun Mats. *Soft Matter* **2012**, *8* (21), 5818–5825. https://doi.org/10.1039/c2sm25557j.